Soil Dynamics and Earthquake Engineering 109 (2018) 286–298

Contents lists available at ScienceDirect

Soil Dynamics and Earthquake Engineering

journal homepage: www.elsevier.com/locate/soildyn

Quantification of model uncertainty and variability in Newmark displacement analysis

Wenqi Du[a], Duruo Huang[b], Gang Wang[c,*]

[a] Institute of Catastrophe Risk Management, Nanyang Technological University, 50 Nanyang Avenue, Singapore
[b] Department of Hydraulic Engineering, Tsinghua University, Beijing, China
[c] Department of Civil and Environmental Engineering, Hong Kong University of Science and Technology, Clear Water Bay, Kowloon, Hong Kong

ARTICLE INFO

Keywords:
Newmark displacement
Model uncertainty
Model variability
Probabilistic analysis

ABSTRACT

Newmark displacement model has been extensively used to evaluate earthquake-induced displacement in earth systems. In this paper, model uncertainty and variability associated with the Newmark displacement analysis are systematically studied. Fourteen Newmark displacement models using scalar or vector intensity measures (IMs) as predictors are compared in this study. In general, model uncertainty for the vector-IM models is found smaller than that of the scalar-IM models, and remains consistent over different earthquake magnitude, distance and site conditions. Yet, the model uncertainty of these Newmark displacement models is still much larger than that of the ground-motion prediction equations (GMPEs) for IMs, indicating further development of the models is much needed. Considering the variabilities contributed from both GMPEs and Newmark displacement models, the total variability of the predicted Newmark displacements is rather consistent among the scalar- and vector-IM displacement models, due to extra sources of variability introduced by incorporating additional IMs. Finally, a logic tree scheme is implemented in the fully probabilistic Newmark displacement analysis to account for the model uncertainty and variability. Sensitivity analysis shows that specific weights would not significantly influence the displacement hazard curves as the results may be dominated by outlier models. Instead, selecting appropriate GMPEs and Newmark displacement models is more important in using the logic-tree framework.

1. Introduction

Since its introduction in the 1960s, Newmark's sliding block [1] and other related models have been widely used to estimate earthquake-induced displacements in natural slopes, earth dams, and solid-waste landfills, *etc*. The Newmark model assumes the sliding mass is rigid during earthquakes, and the deformation of the mass can be neglected. Sliding occurs on a well-defined failure surface when the input acceleration exceeds a critical acceleration (a_c), and the block continues to slide until the relative velocity between the block and ground reaches zero. The permanent displacement of the sliding block, namely the Newmark displacement, is then calculated by integrating the velocity time history of the sliding block (Fig. 1). The critical acceleration a_c represents the resistance of the mass against sliding, and it can be determined by the strength, unit weight of the material and slope angle [2]. The Newmark displacement has been widely used as an index to categorize landslide hazard [3], or to evaluate earthquake-induced shallow sliding in natural slopes, e.g. [4–7].

The first empirical equation to estimate the Newmark displacement was proposed by Newmark [1], which is a function of a_c, peak ground acceleration (PGA) and peak ground velocity (PGV) based on regression analysis of empirical data from four earthquakes. Throughout years, many researchers [8–11] proposed various empirical equations using different ground motion intensity measures (IMs) as predictor variables, including PGA, moment magnitude of the earthquake (M_w), PGV and spectral acceleration (Sa). Arias intensity (Ia) is also a commonly used predictor, as it can effectively incorporate the cumulative effect of an acceleration time history [12,13]. Hence, the Newmark displacement can be predicted based on a single IM, termed as the scalar-IM model, or multiple IMs, termed as the vector-IM model. In general, the vector-IM models are advantageous over the scalar-IM models in that predictions using multiple IMs can better satisfy the efficiency and sufficiency criteria [14]. In other words, a vector-IM model usually yields a smaller standard deviation, which is not much dependent on moment magnitude (M_w) and rupture distance (R_{rup}) of scenario earthquakes. For example, Saygili and Rathje [10] reported that the Newmark models using two IMs generally result in 40–60% reduction in the standard deviations compared with the scalar-IM models.

Recently, Douglas [15,16] and Douglas et al. [17] studied the model uncertainty and consistency of ground motion prediction equations

* Corresponding author.
E-mail address: gwang@ust.hk (G. Wang).

https://doi.org/10.1016/j.soildyn.2018.02.037
Received 4 March 2017; Received in revised form 26 February 2018; Accepted 26 February 2018

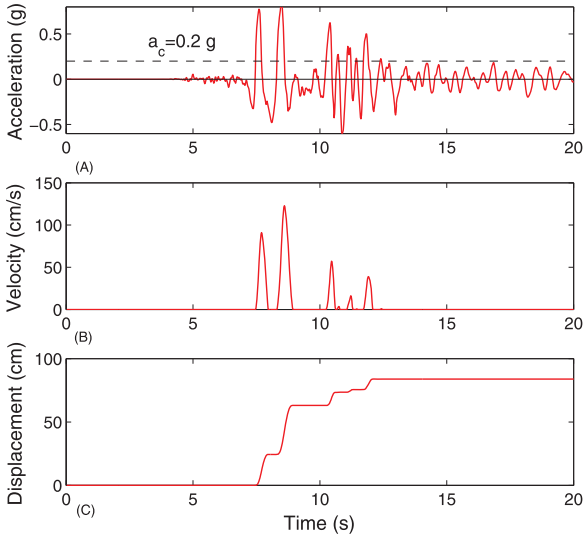

Fig. 1. Computing Newmark displacement with critical acceleration $a_c = 0.2$ g. (A) Earthquake acceleration-time history. (B) Velocity of sliding block versus time. (C) Displacement of sliding block versus time.

(GMPEs) for various IMs (e.g., PGA, PGV, Ia, significant duration) developed during the past four decades. Compared with the ground-motion IMs, two levels of model uncertainties are associated with the Newmark displacement predictions, including uncertainties in the estimation of IMs from GMPEs and uncertainties in the predictions of the Newmark displacement models based on IMs. Because different strong-motion databases and functional forms were used in developing the Newmark displacement models, it is not surprising that these models would yield widely divergent predictions for some scenarios. Yet, uncertainties associated with various levels of the Newmark displacement prediction have not yet been systematically quantified

Uncertainty and variability in a prediction model have been widely discussed in the literature (e.g., [18]). Model uncertainty due to limited knowledge is epistemic. In principal, it can be reduced if more data becomes available or the predictive models are improved. Aleatory variability, on the other hand, represents inherent randomness of the prediction that cannot be reduced. It is usually quantified by the variation of the observed data against model predictions. In this study, uncertainties and variabilities of various Newmark displacement models are quantified under several representative earthquake scenarios. The model uncertainty is approximately evaluated by the dispersion of different prediction models, which employs different predictors, functional forms and databases. The model variability, on the other hand, is approximately by the standard deviation of residuals reported in a prediction model. Although the model variability is reportedly reduced in a vector-IM model as discussed before, inclusion of an additional IM would inevitably induce additional variability associated with the prediction of this IM. Therefore, the total variability of the Newmark displacement prediction is still not clearly studied. The present study will clarify how the model uncertainty and variability in the GMPEs and Newmark models are added up together in the Newmark displacement predictions. Then a logic-tree approach [19] is implemented into a fully probabilistic Newmark displacement analysis [20] to incorporate the uncertainties and variabilities associated with GMPEs and the Newmark displacement models.

2. Selection of Newmark displacement models

In the past, many Newmark displacement models have been proposed by different scholars. A total of eight groups of Newmark models are listed in Table 1. It is seen that the models developed recently (typically later than 2006) were based on much more earthquake events and strong-motion records than earlier models. Fourteen Newmark displacement models proposed since 1988 are used in this study and listed as follows. Among these equations, the unit of the Newmark displacement D is cm; PGA, Sa and a_c are in the unit of g; PGV is in the unit of cm/s; and I_a is in the unit of m/s.

1. [PGA] AM88 model by Ambraseys and Menu [8]:

$$\begin{aligned}\log_{10}(D) &= 0.215 + 2.341\log_{10}\left(1-\frac{a_c}{PGA}\right) - 1.438\log_{10}\left(\frac{a_c}{PGA}\right);\\ \sigma_{\log_{10}D} &= 0.3\end{aligned} \quad (1)$$

2. [PGA Ia] R00 model by Romeo [21]:

$$\begin{aligned}\log_{10}(D) &= 0.607\log_{10}\left(\frac{I_a}{100}\right) - 3.719\left(\frac{a_c}{PGA}\right) + 0.852;\\ \sigma_{\log_{10}D} &= 0.365\end{aligned} \quad (2)$$

3. [PGA, Sa(T = 1)] WA06 model by Watson-Lamprey and Abrahamson [22]:

$$\begin{aligned}\ln D &= (5.47 + 0.451(\ln(S_a(T=1s)) - 0.45)\\ &\quad + 0.0186(\ln(S_a(T=1s)) - 0.45)^2\\ &\quad + 0.596(\ln(A_{RMS}) - 1) + 0.656(\ln(S_a(T=1s)/PGA))\\ &\quad - 0.0716(\ln(S_a(T=1s)/PGA)^2)\\ &\quad + 0.802(\ln(Dur_{a_c}) - 0.74) + 0.0763(\ln(Dur_{a_c}) - 0.74)^2\\ &\quad - \frac{1}{0.581(\ln(PGA/a_c) + 0.193)}\\ \sigma_{\ln D} &= 0.53\end{aligned} \quad (3)$$

where A_{RMS} is the root mean square of acceleration (unit in g) and Dur_{ac} is the duration (unit in s) that the acceleration is greater than the critical acceleration. Prediction equations for A_{RMS} and Dur_{ac} are provided as follows [22]

$$\ln(A_{RMS}(g)) = -1.167 + 1.03\ln(PGA); \quad (4)$$

$$\begin{aligned}\ln(Dur_{a_c}(s)) &= -2.775 + 0.956\ln(PGA/a_c) - \frac{1.554}{\ln(PGA/a_c) + 0.390}\\ &\quad - 0.597\ln(PGA) + 0.381\ln(S_a(T=1s)) + 0.334M_w\end{aligned} \quad (5)$$

4. [PGA] J07 model by Jibson [9]:

$$\log_{10}(D) = 0.215 + 2.341\log_{10}\left(1-\frac{a_c}{PGA}\right) - 1.438\log_{10}\left(\frac{a_c}{PGA}\right);$$

$$\sigma_{\log_{10}D} = 0.51 \quad (6)$$

5. [PGA, M_w] J07 model by Jibson [9]:

$$\begin{aligned}\log_{10}(D) &= -2.71 + 2.335\log_{10}\left(1-\frac{a_c}{PGA}\right) - 1.478\log_{10}\left(\frac{a_c}{PGA}\right)\\ &\quad + 0.424M_w;\\ \sigma_{\log_{10}D} &= 0.454\end{aligned} \quad (7)$$

6. [Ia] J07 model by Jibson [9]:

$$\begin{aligned}\log_{10}(D) &= 2.401\ \log_{10}(I_a) - 3.481\log_{10}(a_c) - 3.23;\\ \sigma_{\log_{10}D} &= 0.656\end{aligned} \quad (8)$$

Table 1
Summary of Newmark displacement models.

Model name	Predictors	No. of earthquakes used	No. of records used	Reference
1. [PGA] AM88	PGA	11 (Ms 6.6–7.2)	50	[8]
2. [PGA Ia] R00	PGA, Ia	17 Italian EQ (M 4.6–6.8)	190	[21]
3. [PGA, Sa(T = 1s)] WA06	PGA, Sa(T = 1s)	(M_w 4.5–7.9)	6158	[22]
4. [PGA] J07	PGA, Ia, M_w	30 (M_w 5.3–7.6)	2770	[9]
5. [PGA, M_w] J07				
6. [Ia] J07				
7. [PGA, Ia] J07				
8. [PGA, M_w] BT07	PGA, M_w	41 (M_w 5.5–7.6)	1376	[23]
9. [PGA] RS08	PGA, Ia, PGV	54 (M_w 5–7.9)	2383	[10]
10. [PGA, Ia] RS08				
11. [PGA, PGV] RS08				
12. [PGA, Ia, PGV] RS08				
13. [PGA, M_w] RS09	PGA, M_w	54 (M_w 5–7.9)	2383	[20]
14. [Ia] HL11	Ia	6 (M_w 6.7–7.6)	1343	[11]

7. [PGA, Ia] J07 model by Jibson [9]:

$$\begin{aligned}\log_{10}(D) &= 0.561\ \log_{10}(I_a) - 3.833\log_{10}\left(\frac{a_c}{PGA}\right) - 1.474;\\ \sigma_{\log_{10}D} &= 0.616\end{aligned} \tag{9}$$

8. [PGA, M_w] BT07 model by Bray and Travasarou [23]:

$$\begin{aligned}\ln(D|D>'0') &= -0.22 - 2.83\ln(a_c) - 0.333(\ln(a_c))^2\\ &\quad + 0.566\ln(a_c)\ln(PGA) + 3.04\ln(PGA)\\ &\quad - 0.244(\ln(PGA))^2 + 0.278(M_w - 7);\\ \sigma_{\ln D} &= 0.66\end{aligned} \tag{10}$$

Note that the above prediction is only for "nonzero" displacements ($D > 1$ cm). The probability of "zero" displacements ($D \leq 1$ cm) can be estimated as

$$P(D = "0") = 1 - \Phi(-1.76 - 3.22\ln(a_c) + 3.52\ln(PGA)) \tag{11}$$

Finally, the median (50th percentile) displacement is determined and used in subsequent analyses:

$$\ln D = \ln(D|D > "0") + \sigma_{\ln D} \times \Phi^{-1}\left(1 - \frac{0.5}{[1 - P(D = "0")]}\right) \tag{12}$$

9. [PGA] RS08 model by Saygili and Rathje [10]:

$$\begin{aligned}\ln D &= 5.52 - 4.43\left(\frac{a_c}{PGA}\right) - 20.39\left(\frac{a_c}{PGA}\right)^2 + 42.61\left(\frac{a_c}{PGA}\right)^3\\ &\quad - 28.74\left(\frac{a_c}{PGA}\right)^4 + 0.72\ln(PGA);\\ \sigma_{\ln D} &= 1.13\end{aligned} \tag{13}$$

10. [PGA, Ia] RS08 model by Saygili and Rathje [10]:

$$\begin{aligned}\ln(D) &= 2.39 - 5.24\left(\frac{a_c}{PGA}\right) - 18.78\left(\frac{a_c}{PGA}\right)^2 + 42.01\left(\frac{a_c}{PGA}\right)^3\\ &\quad - 29.15\left(\frac{a_c}{PGA}\right)^4 - 1.56\ln(PGA) + 1.38\ln(I_a);\\ \sigma_{\ln D} &= 0.46 + 0.56(a_c/PGA)\end{aligned} \tag{14}$$

11. [PGA, PGV] RS08 model by Saygili and Rathje [10]:

$$\begin{aligned}\ln D &= -1.56 - 4.58\left(\frac{a_c}{PGA}\right) - 20.84\left(\frac{a_c}{PGA}\right)^2 + 44.75\left(\frac{a_c}{PGA}\right)^3\\ &\quad - 30.5\left(\frac{a_c}{PGA}\right)^4 - 0.64\ln(PGA) + 1.55\ln(PGV);\\ \sigma_{\ln D} &= 0.41 + 0.52(a_c/PGA)\end{aligned} \tag{15}$$

12. [PGA, Ia, PGV] RS08 model by Saygili and Rathje [10]:

$$\begin{aligned}\ln(D) &= -0.74 - 4.93\left(\frac{a_c}{PGA}\right) - 19.91\left(\frac{a_c}{PGA}\right)^2 + 43.75\left(\frac{a_c}{PGA}\right)^3\\ &\quad - 30.12\left(\frac{a_c}{PGA}\right)^4 - 1.3\ln(PGA) + 1.04\ln(PGV) + 0.67\ln(I_a);\\ \sigma_{\ln D} &= 0.2 + 0.79(a_c/PGA)\end{aligned} \tag{16}$$

13. [PGA, M_w] RS09 model by Rathje and Saygili [20]:

$$\begin{aligned}\ln(D) &= 4.89 - 4.85\left(\frac{a_c}{PGA}\right) - 19.64\left(\frac{a_c}{PGA}\right)^2 + 42.49\left(\frac{a_c}{PGA}\right)^3\\ &\quad - 29.06\left(\frac{a_c}{PGA}\right)^4 + 0.72\ln(PGA) + 0.89(M_w - 7);\\ \sigma_{\ln D} &= 0.73 + 0.79(a_c/PGA) - 0.54(a_c/PGA)^2\end{aligned} \tag{17}$$

14. [Ia] HL11 model by Hsieh and Lee [11]:

$$\begin{aligned}\log_{10}(D) &= 0.847\log_{10}(I_a) - 10.62a_c + 6.587a_c\log_{10}(I_a) + 1.84;\\ \sigma_{\log_{10}D} &= 0.295\end{aligned} \tag{18}$$

In the above models, the [PGA] AM88, [PGA] J07, [PGA, M_w] J07, [Ia] J07, [PGA, M_w] BT07, [PGA] RS08, [PGA, M_w] RS09 and [Ia] HL11 models employ only a single IM (PGA or Ia) as the predictor, so they are grouped as the scalar-IM models. The M_w term appears in some of these scalar-PGA models to eliminate biases against the earthquake magnitude. The other six models employ multiple IMs (i.e., PGA, Ia, Sa(T = 1 s) or PGV), and then they are categorized as the vector-IM models. It is worth mentioning that the [Ia] J07 and the [Ia] HL11 models only employ Ia as the predictor, which might provide biased estimates when ground motions are small, since a small but finite displacement will still be predicted by the scalar-Ia model even if the PGA is smaller than a_c.

3. Model uncertainty and variability in the Newmark displacement predictions

3.1. Model uncertainty of predicted Newmark displacements

Model uncertainty of the above Newmark models is studied by comparing the difference of the median predicted displacements for a given earthquake scenario. Earthquake scenarios considered in the analysis are earthquakes with moment magnitude (M_w) of 7.5, 6.5 and 5.5 occurred on a strike-slip fault. The site conditions are assumed to be a stiff-soil site and a rock site, where the time-averaged shear wave velocity of the top 30 m (V_{s30}) are 400 m/s and 760 m/s, respectively. Four Next Generation Attenuation (NGA) GMPEs [24–27] are used to

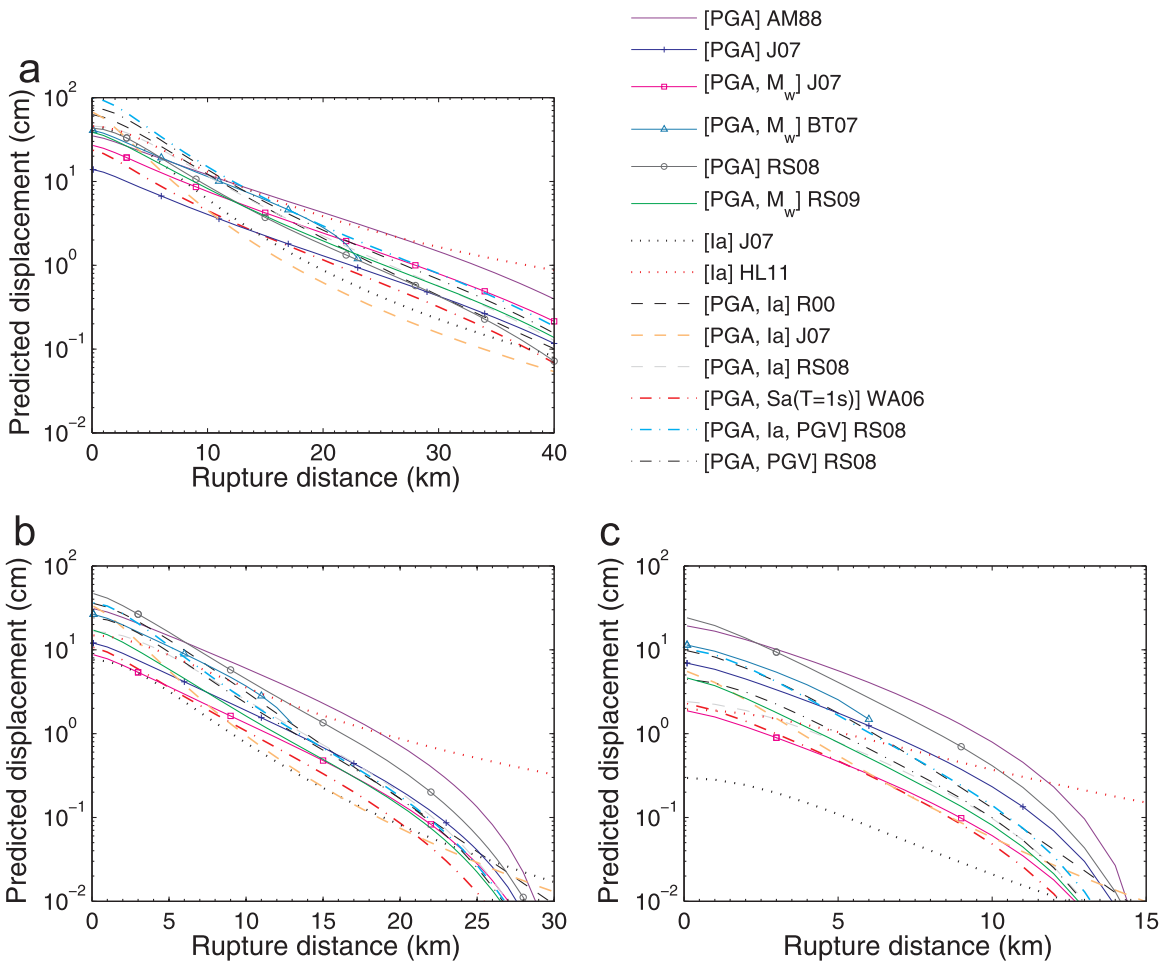

Fig. 2. Median predicted displacements by various Newmark models for (a) M_w = 7.5, (b) M_w = 6.5, and (c) M_w = 5.5, strike-slip events. a_c = 0.1 g, V_{s30} = 400 m/s. Note: for each scenario, the average of the predicted median IMs are used as input parameters.

predict PGA, PGV, and response spectral acceleration at 1 s Sa(T = 1 s), respectively. The GMPEs proposed by Travasarou *et al.* [28], Foulser-Piggott and Stafford [29], and Campbell and Bozorgnia [30] are chosen for predicting Ia. In order to eliminate the influence of model uncertainty and variability existed in these GMPEs, the averaged values of the median predictions of various GMPEs are adopted as the inputs to estimate the median Newmark displacements.

Figs. 2 and 3 show the median predicted Newmark displacements versus rupture distances for the soil sites and rock sites with a_c = 0.1 g. Three strike-slip earthquake scenarios with M_w = 7.5, 6.5 and 5.5 are considered in these plots. It can be observed that the predicted displacements by different Newmark displacement models vary significantly for a given earthquake scenario. For example, the estimated median displacements in Fig. 2(a) range from 4 cm to 18 cm for M_w 7.5 at a rupture distance of 10 km. Model uncertainty is expected to be higher if the predicted median displacements among these models are more scattered. As seen from these plots, the predicted median displacements (in natural logarithmic scale) are more scattered as rupture distance increases, especially for the M_w 5.5 event. Since very small displacement amplitudes are of little engineering significance, it is more rational to focus only on large displacement amplitudes. For the M_w 5.5 scenario, it can also be observed that the two scalar-Ia models ([Ia] J07, [Ia] HL11) exhibit systematically different trends compared with the other models. As explained previously, the scalar-Ia models might provide biased estimates for the small-amplitude ground motions compared with the other models.

Fig. 4 shows the corresponding standard deviations of logarithmic predicted median displacement (shown in Figs. 2 and 3) for the soil sites and rock sites. Note that the data is only plotted for the rupture distance up to 30 km, 20 km and 10 km for M_w = 7.5, 6.5, 5.5, respectively. The displacement data within this range is generally greater than 0.1 cm. The standard deviations would become significantly larger for longer rupture distances, yet the displacements are small and of little engineering importance. For the scalar models, the model uncertainty for the large-magnitude events is generally smaller than that of the small-magnitude events. The standard deviations of the ln(D) predicted by the scalar models are approximately in the range of 0.4–1.0 for M_w 7.5 and 6.5, and 1.2–1.7 for M_w 5.5. This is not unexpected since the number of moderate-to-large magnitude events (M_w > 6) is usually dominant in the strong-motion databases that have been used to develop the Newmark displacement models. It is also worth mentioning that for the scalar models, the standard deviations in the rock site are up to 25% larger than that of the soil site. Because the displacement models were usually developed from strong motions recorded mostly on soil sites. The scalar models based on PGA inherently predict displacements representative of lower V_{s30} motions. Therefore, application of the scalar model to the rock site involves larger uncertainty.

On the other hand, the model uncertainties associated with vector models are generally smaller than those of the scalar models for most cases, as shown in Fig. 4. The standard deviations of ln(D) for the vector models fall into a narrow range (0.4–0.6) for all these M_w, R and Vs_{30} considered, implying that the model uncertainties associated with vector models are quite consistent for all cases because the vector IMs

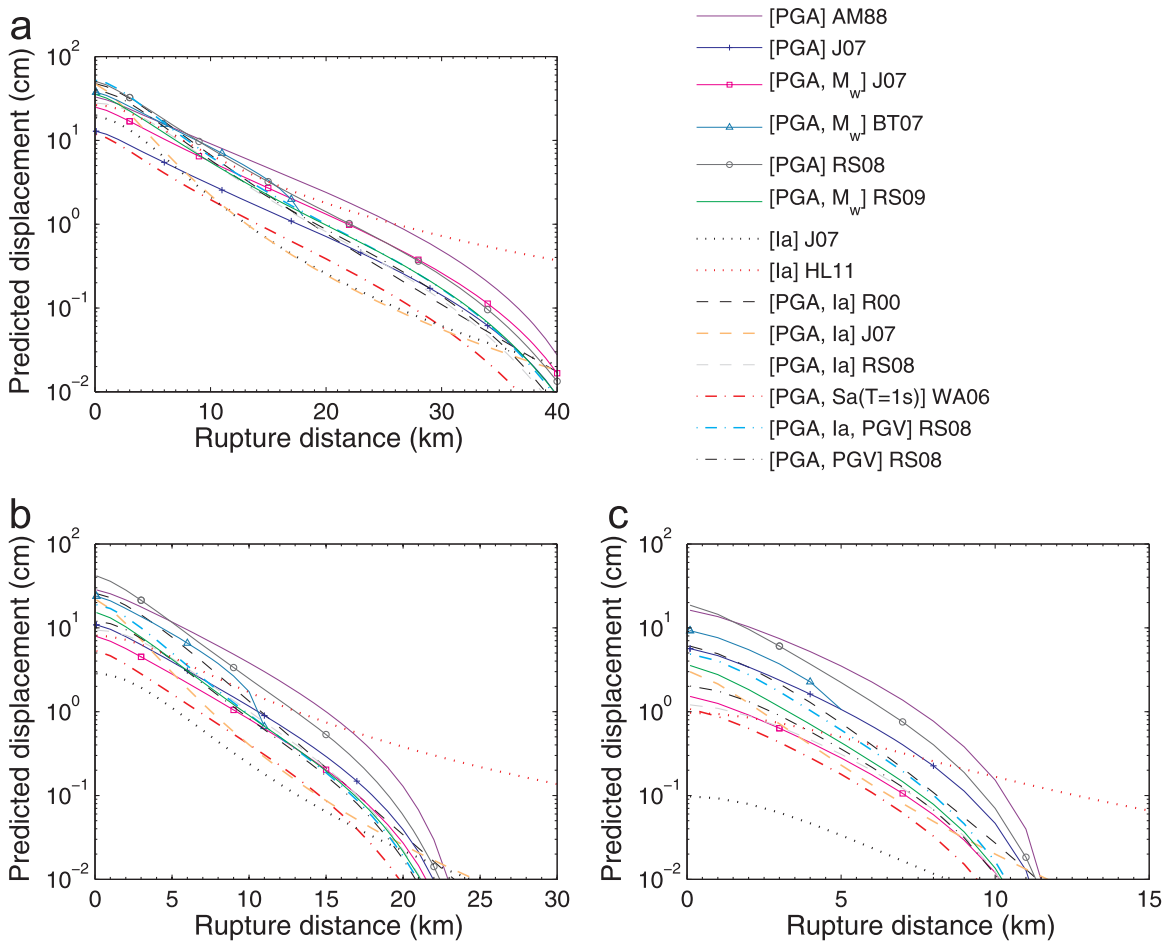

Fig. 3. Median predicted displacements by various Newmark models for (a) M_w = 7.5, (b) M_w = 6.5, and (c) M_w = 5.5, strike-slip events. a_c = 0.1 g, V_{s30} = 760 m/s. Note: for each scenario, the average of the predicted median IMs are used as input parameters.

represent different aspects of ground motion characteristics. To put it simple, the second IM in a vector (either Ia or PGV) is important to characterize the frequency content of ground motions. When only PGA is used in a scalar model, it is difficult to distinguish between a near-field M_w 6 motion on rock versus a far-field *Mw* 7.5 motion on soil, since they may have the same PGA but very different frequency contents. The second IM allows one to distinguish these motions. Therefore, uncertainties estimated for the rock site and the soil site are consistent using the vector models.

Furthermore, the model uncertainties in both the GMPEs and Newmark displacement models are considered collectively in the subsequent analysis. Instead of applying the averaged median IMs to compute the Newmark displacements as before, the median predicted IM from each individual GMPE (i.e., one from the four NGA models for PGA, PGV; one from the three GMPEs for Ia) is used to compute the median displacements of all the 14 Newmark displacement models without differentiating the scalar and the vector models for the soil site, as shown in Fig. 5. Altogether, there are 168 (4 × 3 × 14) combinations of GMPEs and displacement models in each subplot. The predicted Newmark displacements are significantly scattered, indicating that the selection of specific GMPEs and Newmark displacement models would considerably influence the final results. For example, the estimated median displacements range from 2 cm to 40 cm for M_w 7.5 at the rupture distance of 10 km.

Fig. 6 shows the corresponding standard deviations of the displacements $\sigma_{\ln D}$. The standard deviations by considering both model uncertainties in GMPEs and Newmark displacement models is generally 0.2–0.4 larger than the previous analysis by considering only the displacement model uncertainty. The results are generally consistent with the reported standard deviations of the model uncertainties for PGA, PGV and Ia, which are approximately 0.2–0.4 on the natural logarithmic scale [15,16]. The model uncertainty of the Newmark displacement models appears to be much larger than those of the GMPEs, probably due to the inherent difficulty in correlating the Newmark displacements with IMs by using simple function forms. It then calls for more research effort to develop advanced Newmark displacement models in the future. In summary, the standard deviations of model uncertainties considering both the input IMs and Newmark displacements are approximately 0.6–1 for larger magnitude events (M_w > 6) and 1.3–1.5 for smaller magnitude events (M_w < 6), all represented on a natural logarithmic scale. The large standard deviations imply that both of the two levels of model uncertainties should be well quantified in the Newmark displacement analysis.

3.2. Model variability of predicted Newmark displacements

In this subsection, the model variability of the Newmark displacement models is compared for different earthquake scenarios. Although the vector-IM models usually reported smaller standard deviations ($\sigma_{\ln D}$) compared with the scalar-IM models, inclusion of additional IMs as predictors may also introduce extra variability in the IMs themselves. Therefore, the total variability of the Newmark displacement for an earthquake scenario should account for the contribution of variability in GMPEs and variability in Newmark displacement models.

Monte-Carlo simulation is used herein to evaluate the total variability of the estimated Newmark displacement. Firstly, 100 sets of

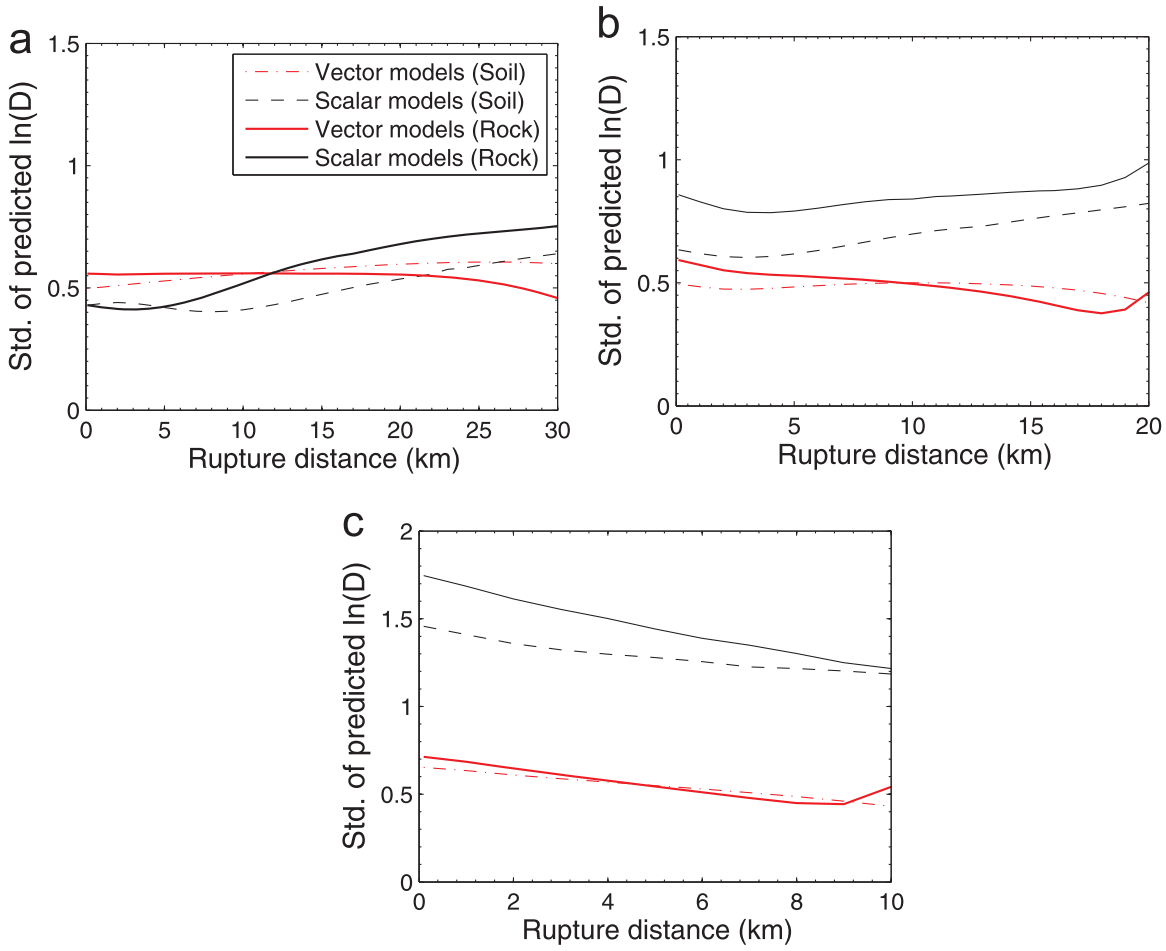

Fig. 4. Standard deviations of the median predicted Newmark displacements (in natural log scale) by different models, for (a) M_w = 7.5, (b) M_w = 6.5, (c) M_w = 5.5, strike-slip events. The site condition is rock (V_{s30} = 760 m/s) or soil (V_{s30} = 400 m/s).

properly correlated vector IMs are generated for a given earthquake scenario. The vector IMs are assumed to follow a multivariate lognormal distribution with means and standard deviations specified by GMPEs. For the vector-IM models, the joint occurrence of multiple IMs can be specified by the empirical correlations between the residuals of IMs. A strong positive correlation coefficient ρ_{IM_1,IM_2} indicates that large values of IM_1 are closely in association with large values of IM_2. The correlation coefficients among PGA, PGV, Ia and Sa(T = 1 s) are obtained from previous studies and listed in Table 2. Secondly, for each set of vector IMs, 100 Newmark displacement values are simulated by assuming that the displacements follow a lognormal distribution, with the mean and standard deviation ($\sigma_{\ln D}$) specified by the Newmark displacement models. The standard deviation of the resulting 10,000 displacement values is then calculated to estimate the total variability for each Newmark displacement model. It is noted that very small displacement values have to be excluded, because they are of little engineering importance, but appear to be highly scattered on the logarithmic scale. In this study, only displacement values greater than 0.01 cm are considered.

Figs. 7 and 8 show the obtained total standard deviations versus rupture distances for M_w 6.5 and M_w 7.5 strike-slip events using various Newmark displacement models. The averaged $\sigma_{\ln PGA}$ obtained from four NGA models is also plotted in Fig. 7(e) for comparison. The standard deviations of the predicted Newmark displacements have quite similar trend for all scenarios, which generally falls into 1.5–2 at short rupture distances and remains around 2 when R > 10 km. Note that exclusion of displacements smaller than the cutoff value (0.01 cm) reduces the data scatter artificially, and results in a slightly decreasing trend at larger distances, which is the case particularly for Fig. 8(b). The total variabilities are significantly larger than the reported $\sigma_{\ln D}$ in the Newmark displacement models. For example, although the reported standard deviation of the [Ia] HL11 model is 0.295 on $\log_{10}$ scale (0.68 in natural logarithmic scale), the total standard deviations of Newmark displacements are as high as 1.5, due to the large variability for predicting Ia ($\sigma_{\ln Ia} \approx 1$).

It is also important to note that, in general, there is no systematic difference in the total variabilities between the scalar and vector models. This is actually an encouraging result since the total variability represents the inherent randomness, which, in principle, should not vary significantly from model to model. Yet, [Ia] J07 and [PGA, Ia] J07 appear to have quite different trend than all other models. As shown in Eqs. (8)(9), the standard deviations of these two models are substantially larger than others ($\sigma_{\log_{10}D}$ = 0.656 and 0.616 is equivalent to $\sigma_{\ln D}$ = 1.51 and 1.42), which results in high standard deviations at short distances in Figs. 7 and 8. On the other hand, these two models predict relatively low displacements shown in Figs. 2 and 3. Therefore, they are mostly affected by data cutoff and standard deviation shows a decreasing trend over the rupture distance.

4. Probabilistic Newmark displacement analysis

4.1. Displacement hazard curve

In engineering practice, Newmark displacements are usually estimated based on a pseudo-probabilistic approach: first, the hazard curves of IMs are generated from conventional probabilistic seismic

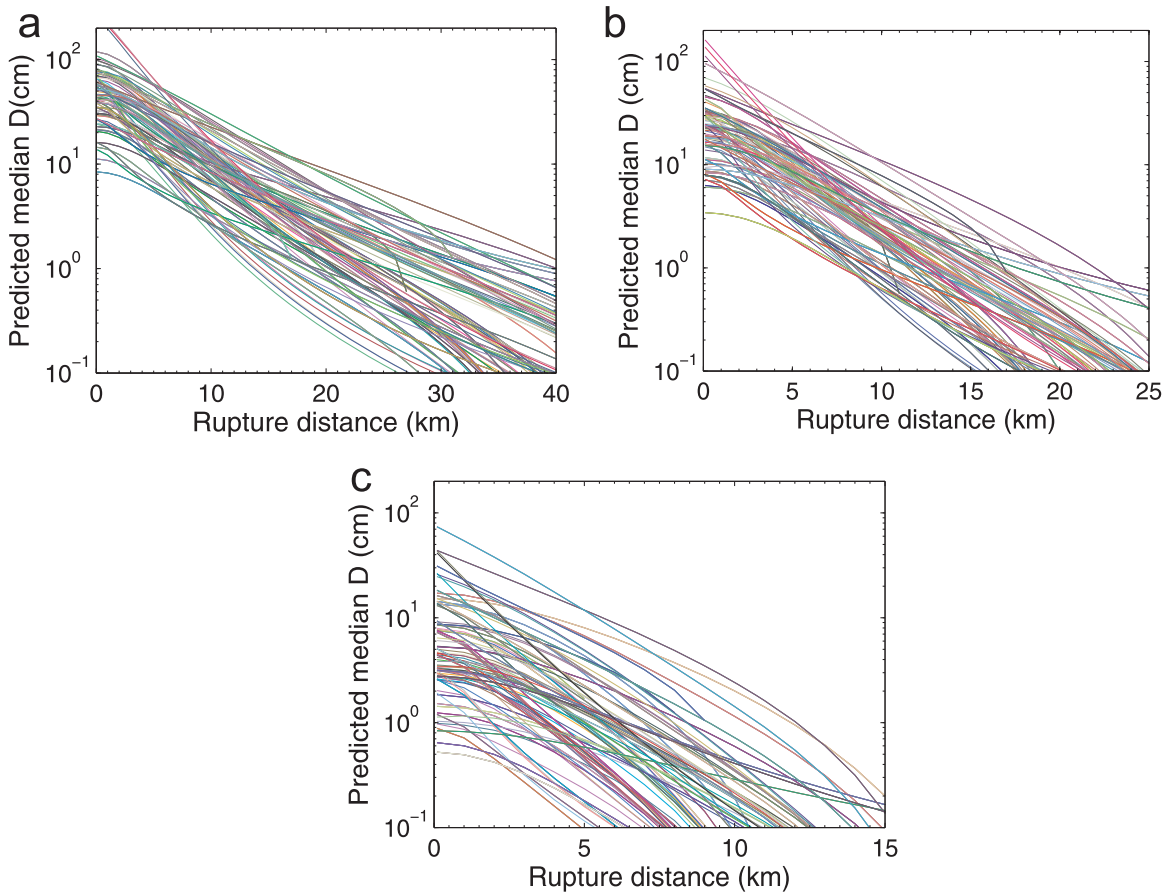

Fig. 5. Variation of median displacements predicted by various GMPEs and Newmark displacement models, for (a) $M_w = 7.5$, (b) $M_w = 6.5$, and (c) $M_w = 5.5$, strike-slip events, $a_c = 0.1$ g, $V_{s30} = 400$ m/s.

hazard analysis (PSHA); second, the corresponding IM value at a certain hazard level (e.g., a return period of 500 years) is used as input to compute the Newmark displacement. The significant limitation of the pseudo-probabilistic approach is that, the annual rate of exceedance of the computed displacement remains unknown. On the other hand, fully probabilistic Newmark displacement analysis [7,34] provides the annual rate of exceedance of the Newmark displacement directly. The fully probabilistic seismic displacement approach accounts for the model variabilities in both IMs and the Newmark displacements. The procedure will be briefly described below.

In conventional PSHA, the mean annual rate of exceedance of an IM can be determined as:

$$\lambda_{IM}(z) = \lambda_0 \int_m \int_r P[IM > z|m, r] f(m) f(r) dm dr \tag{19}$$

where $\lambda_{IM}(z)$ refers to the mean annual rate of an IM exceeding a given value of z (also called the IM hazard curve); λ_0 is the activity rate of the source; $f(m)$ and $f(r)$ represent the probability density functions of earthquake magnitude m and site-to-source distance r, respectively. $P[IM > z|m, r]$ denotes the probability of IM exceeding z value, given an earthquake scenario (m, r). This term can be obtained from GMPEs. Accordingly, the derivative of the IM hazard curve, $f_{\mathrm{IM}}(z)$, which represents the mean annual rate density of a scalar IM $= z$, is computed as [35]:

$$f_{\mathrm{IM}}(z) = \frac{d(\lambda_{IM}(z))}{dz} = \lambda_0 \int_m \int_r f_{IM}(z|m, r) f(m) f(r) dm dr \tag{20}$$

where $f_{IM}(z|m, r)$ refers to the lognormal probability density function of an IM, given m and r:

$$f_{IM}(z|m, r) = \frac{1}{z\sigma_{\ln IM}\sqrt{2\pi}} \exp\left\{\frac{-(\ln z - \mu_{\ln IM})^2}{2\sigma_{\ln IM}^2}\right\} \tag{21}$$

Similar to the above PSHA analysis, the mean annual rate of exceedance λ_D for the Newmark displacement value D can be represented as:

$$\lambda_D(x) = \int P[D > x|IM = z] \cdot f_{\mathrm{IM}}(z) dz \tag{22}$$

where $\lambda_D(x)$ is mean annual rate of D exceeding a given value x; $P[D > x|IM = z]$ denotes the probability that a displacement value x is exceeded for a given IM value z, as computed by the scalar-IM Newmark model; $f_{\mathrm{IM}}(z)$ is the probability of occurrence of IM $= z$, as computed by Eq. (20).

If two IMs are used in the Newmark models, the joint probability density function of these two IMs need to be well addressed [35]. The displacement hazard curve is calculated as:

$$\lambda_D(x) = \int P(D > x|\mathrm{IM}_1 = y, \mathrm{IM}_2 = z) f_{\mathrm{IM}_1,\mathrm{IM}_2}(y, z) dz dy \tag{23}$$

where $f_{\mathrm{IM}_1,\mathrm{IM}_2}(y, z)$ is the joint probability of occurrence for $\mathrm{IM}_1 = y$ and $\mathrm{IM}_2 = z$. It is worth mentioning that the correlation coefficient between two IMs, as shown in Table 2, is required to get the joint probability density function $f_{\mathrm{IM}_1,\mathrm{IM}_2}(y, z)$. Eqs. (22) and (23) can be used to derive the displacement hazard curves analytically using a single IM or two IMs, respectively. The analytical procedure would be more complicated if more than 3 IMs are involved. Therefore, we will limit the following analysis to the scalar-IM models and the vector models with 2 IMs.

The two levels of model variabilities (i.e., $\sigma_{\ln IM}$ and $\sigma_{\ln D}$) can be fully incorporated in the above analytical procedures. Model uncertainty, on the other hand, can be accounted for by a logic-tree

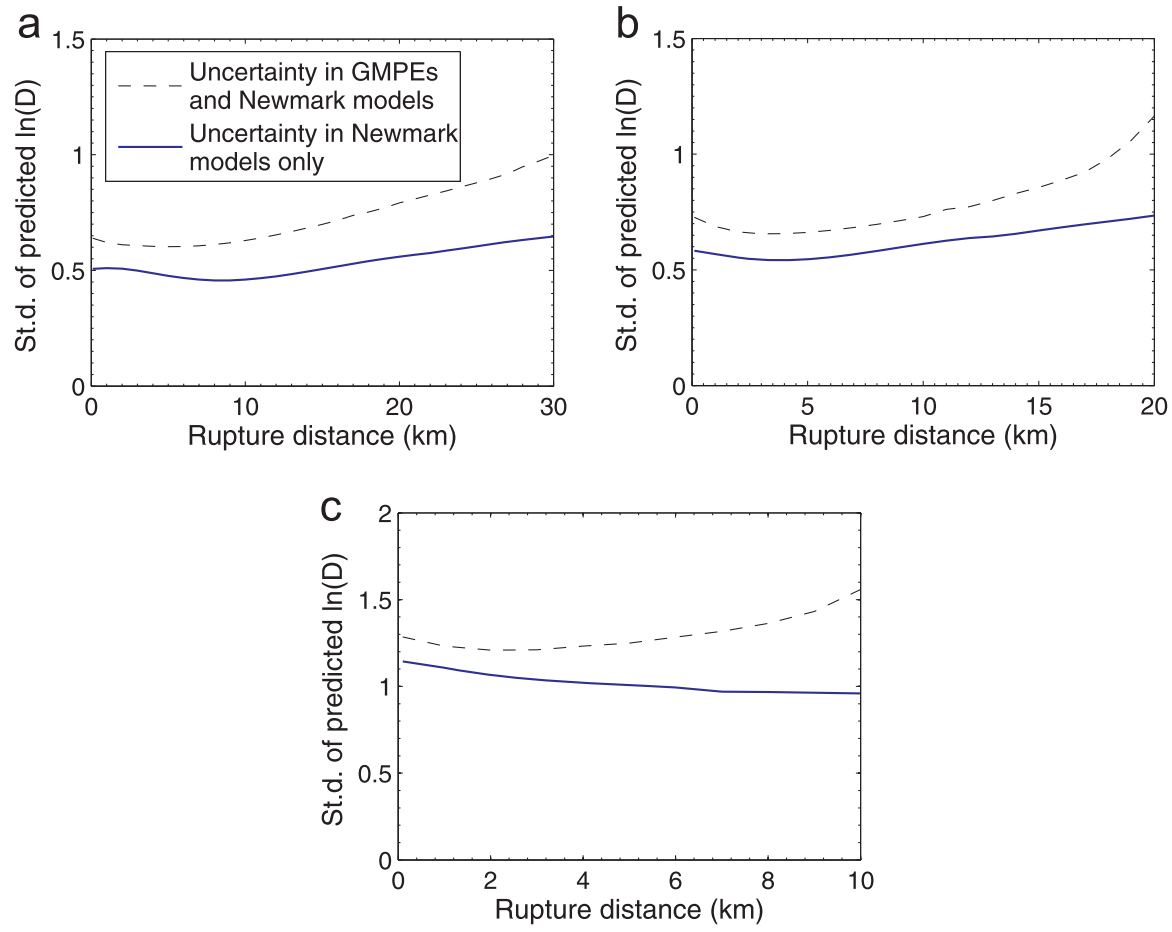

Fig. 6. Standard deviations of predicted Newmark displacements (on natural logarithmic scale) considering uncertainties in both GMPEs and Newmark displacement models, or only in Newmark displacement models, for (a) M_w = 7.5, (b) M_w = 6.5, and (c) M_w = 5.5, strike-slip events, a_c = 0.1 g, V_{s30} = 400 m/s.

Table 2
Correlation coefficients between the IMs used in Newmark displacement models.

IMs	PGA	Ia	PGV	Sa(T = 1s)
PGA	1	0.88	0.69	0.53
Ia	0.88	1	0.74	0.7
PGV	0.69	0.74	1	0.77
Sa(T = 1s)	0.53	0.7	0.77	1

Note: the following references are used to obtain the correlation coefficients: ρ(PGA, Ia), ρ(PGA, PGV) and ρ(Ia, PGV) [30]; ρ(PGA, Sa(T = 1 s)) [31]; ρ(Ia, Sa (T = 1 s)) [32] and ρ(PGV, Sa(T = 1 s)) [33].

framework. The logic-tree approach has been widely used in PSHA to capture the uncertainties in seismic sources and GMPEs (e.g., [36]). Logic-tree branch weights need to be assigned to represent the confidence or the acceptance of specific models. Issues related to logic trees and weighting schemes in PSHA have been discussed in previous studies (e.g., [37–39]). One important requirement for an appropriate logic tree is that the selected prediction models should be both mutually exclusive and collectively exhaustive [37]. The "mutually exclusiveness" requires the selected model at each logic-tree branch to be different in theory (without model redundancy), and the "collectively exhaustiveness" requires that one of the models should be implicitly "true". In other words, logic trees should incorporate all appropriate models, and the models in logic-tree branches should be independent with each other. Hence, to remove model redundancy, it would be desirable if only one Newmark displacement model is selected from each publication to build the logic-tree framework.

4.2. Illustrative examples

To demonstrate the probabilistic Newmark displacement analysis with logic-tree branches, three hypothetical slopes with critical acceleration a_c as 0.05 g, 0.1 g and 0.2 g are considered. The slopes are located on a stiff soil site (V_{s30} = 400 m/s), at a rupture distance of 10 km from a point source. The seismicity of the source is assumed to follow the Gutenberg-Richter relationship as:

$$\log_{10}\lambda_m = 4.4 - 1.0M_w \tag{24}$$

where λ_m is the mean annual rate of exceedance of the moment magnitude M_w. The minimum and maximum magnitudes are set as 4.4 and 7.5, respectively. A total of 31 magnitude scenarios with a magnitude bin of 0.1 are sampled. The aforementioned GMPEs are used in the PSHA procedure to compute the hazard curves of PGA and Ia at the site, as shown Fig. 9. It can be seen that using different GMPEs would result in considerably different hazard curves. For instance, the PGA values at λ_{IM} = 0.0021(i.e., 10% probability of exceedance in 50 years) are in the range of 0.53 g to 0.87 g. The mean hazard curve is also plotted in Fig. 9 by averaging the computed IMs of different models at each hazard level.

Based on the aforementioned fully probabilistic displacement hazard procedures, the displacement hazard curves are calculated and compared in Fig. 10 using seven selected scalar- and vector-IM models for slopes with a_c values as 0.05, 0.1 and 0.2 g, respectively.

These seven models are selected based on the consideration of "mutually exclusiveness" and "collectively exhaustiveness" requirements as discussed before, including three scalar-PGA models, one scalar-Ia model and three vector [PGA, Ia] models. Newmark displacement models employing three IMs are not considered herein due

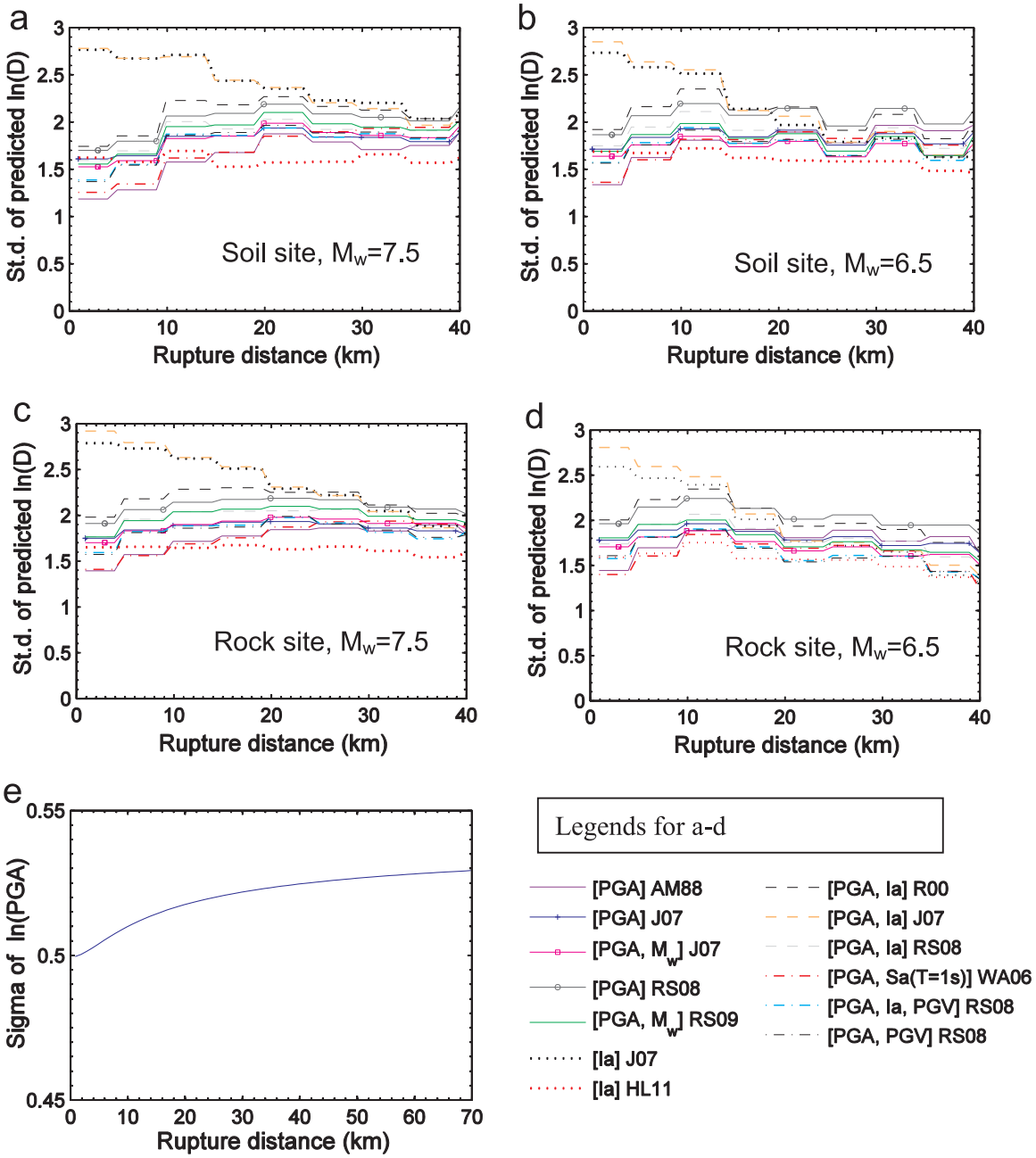

Fig. 7. Standard deviations of the predicted Newmark displacements considering variabilities in GMPEs and Newmark displacement models, for (a) M_w = 7.5 and (b) M_w = 6.5 strike-slip events, V_{s30} = 400 m/s, (c) M_w = 7.5 and (d) M_w = 6.5 strike-slip events, V_{s30} = 760 m/s. The cut-off displacement value is 0.01 cm, a_c = 0.1 g. (e) Standard deviations of ln(PGA).

to its complexity involved in the analytical procedure. At the return periods generally considered in engineering applications (i.e., 500–2500 years), the [PGA Ia] RS08 model gives the lower bound of the displacement hazard curves, whereas the [PGA Ia] J07 and [PGA Ia] R00 models yield the upper bound. Fig. 10 clearly highlights significant model divergence in the probabilistic Newmark displacement analysis. For the case of a_c = 0.1 g (Fig. 10 b), the Newmark displacements at the 1000 years return period (λ_D = 0.001) are approximately in the range of 60–300 cm. The range of scatter becomes more significant at higher hazard levels ($\lambda_D \leq 0.001$), implying that great model uncertainty is involved. Besides, it can be observed that the mean displacement hazard curve is largely affected by models with the highest displacement estimates, in particular, the [PGA Ia] J07 model. The results would be more consistent if this model is not selected.

Another issue related to the logic-tree analysis is how to distribute the weights among the selected models in the analysis. The logic-tree weights are generally assigned based on expert judgments or model rankings. To test the sensitivity of weighting schemes in the displacement hazard analysis, six different weighting schemes are used. The details of each weighting scheme are summarized in Table 3. They include: equal weights, four experts' weighting schemes and random weights. Expert 1 preferentially weighted the models proposed recently (later than 2007); Expert 2 preferentially weighted the vector-IMs (PGA and Ia) models; Expert 3 only selected and equally weighted the PGA-based models, which is applicable for cases where Ia is difficult to predict. The weights of Expert 4 were ranked based on the relative accuracy of these displacement models, and the reported standard deviation $\sigma_{\ln D}$ of each model was used to arrange the sequences.

The displacement hazard curves for various a_c cases considering different weightings are shown in Fig. 11. It can be seen that except for

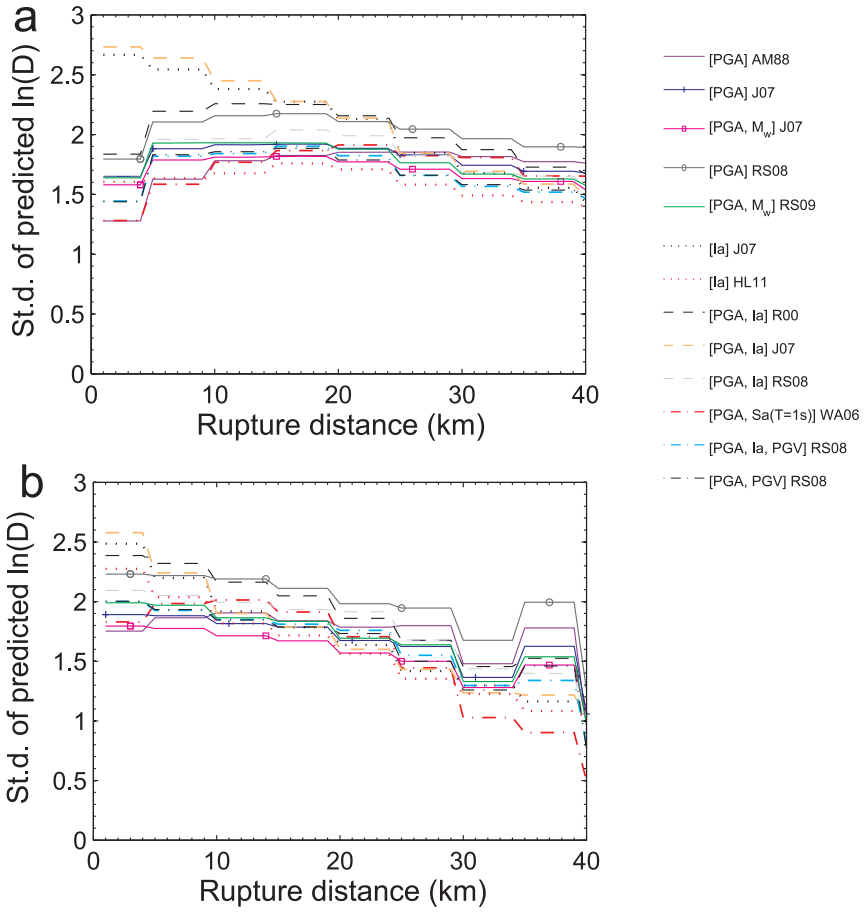

Fig. 8. Standard deviations of the predicted Newmark displacements considering variabilities in GMPEs and Newmark displacement models, for (a) $M_w = 7.5$ and (b) $M_w = 6.5$, strike-slip events, $V_{s30} = 400$ m/s. The cut-off displacement value is 0.01 cm, $a_c = 0.2$ g.

Expert 3's weights, where only three PGA-based models are employed and all other vector-IM models are neglected, the overall curves are generally consistent, even for the case of random weights. This indicates that the specific weighting schemes would not notably influence the resulting displacement hazard curves, while the selection of proper displacement models seems to play a more important role. Therefore, more attention should be drawn to establishing appropriate branches (models) of the logic-tree framework rather than assigning specific weight to each branch. This result corroborates with findings from other scholars [40,41].

It is also interesting to compare some of the displacement hazard curves. As shown in Fig. 10, three vector [PGA Ia] models developed by different researchers clearly show quite divergent results. On the other hand, the displacement hazard curves developed by the same authors using the same strong motion database appear to be quite consistent, as is clearly illustrated in Fig. 12 for the scaler model, [PGA M_w] RS09, and two vector models, [PGA Ia] RS08 and [PGA PGV] RS08. Therefore, the performance of the Newmark displacement models is mainly

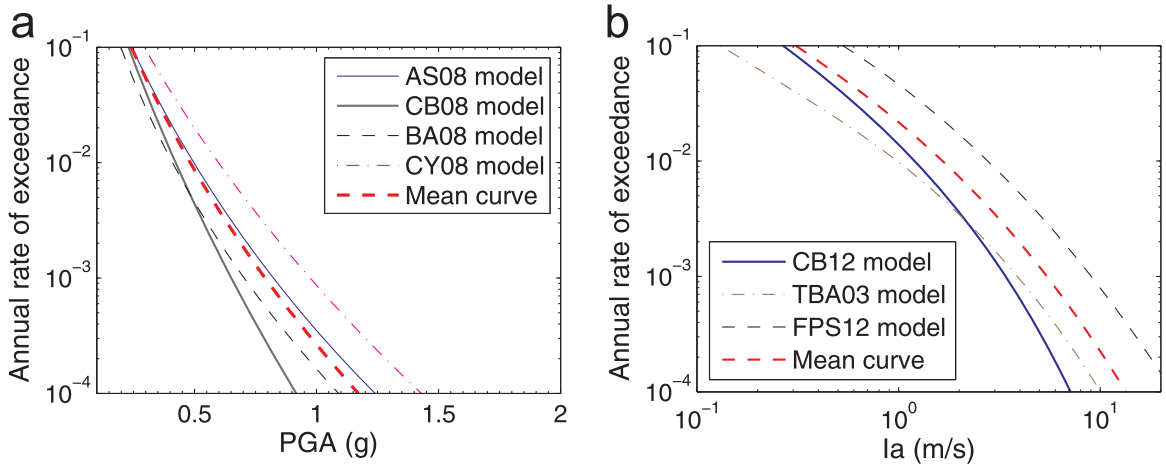

Fig. 9. Hazard curves for ground-motion IMs using different GMPEs. (a): PGA hazard curves using four GMPEs: AS08 [24], BA08 [25], CB08 [26] and CY08 [27], respectively. (b): Ia hazard curves using three GEMPs: TBA03 [28], FPS12 [29] and CB12 [30].

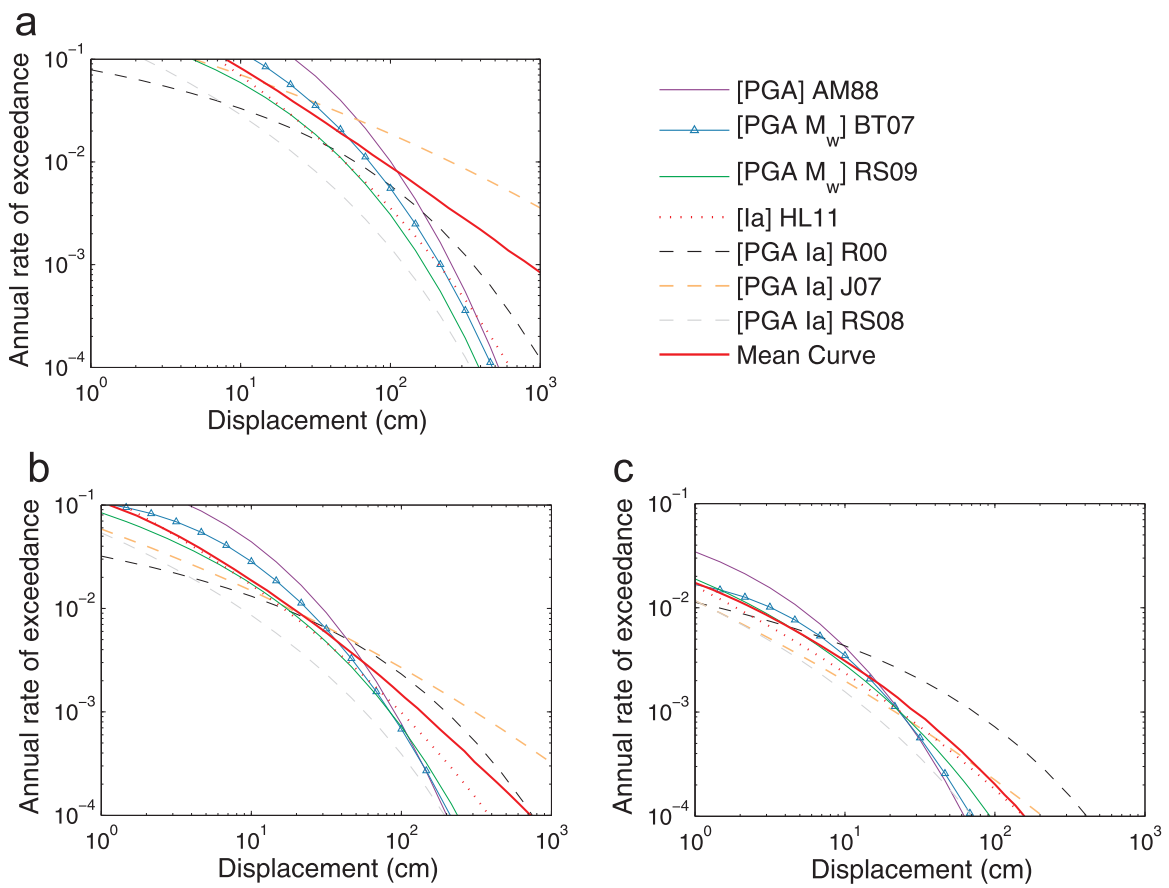

Fig. 10. Displacement hazard curves using different Newmark models for three cases: (a) $a_c = 0.05$ g, (b) $a_c = 0.1$ g and (c) $a_c = 0.2$ g.

dependent on the ground-motion database and functional forms used, rather than specific IMs employed as predictors.

5. Discussions and conclusions

In this paper, the model uncertainties and variabilities associated with the Newmark displacement analysis are systematically studied. A total of fourteen Newmark models using scalar- and vector-IMs are selected from eight publications in this study. The model uncertainty of the Newmark models is first assessed by examining the distribution of median displacement predictions under scenario earthquakes. The standard deviations of the model uncertainty in these scalar Newmark displacement models are within 0.4–1.0 for large events, and 1.2–1.7 for small events on a natural logarithmic scale. The standard deviations for vector models are quite consistently within 0.4–0.6. If the model uncertainty in the GMPEs is also considered, the standard deviations would generally increase by 0.2–0.4. The results indicate the model uncertainty contributed from the Newmark displacement models alone is significantly larger than that in GMPEs. More effort should be devoted to developing advanced Newmark displacement models to reduce the model uncertainty in the future.

The total variability of the predicted Newmark displacements is also studied for some representative earthquake scenarios. Considering both the model variabilities in the GMPEs and the Newmark displacement models, the total standard deviations of the predicted displacements are found to be 1.5–2 on natural logarithmic scale if the cutoff value is chosen as 0.01 cm. It is found that the model variabilities are rather consistent among the scalar- and vector-IM models. Using vector IMs does not significantly reduce the total variability of the predicted displacements, due to extra sources of variability introduced by incorporating additional IMs. However, the model uncertainty for the vector-IM models is generally smaller than that of the scalar models. Another advantage of using vector IMs is that the vector-IM models can better satisfy the sufficiency criterion [14]. For scalar-IM models, M_w should be incorporated to eliminate bias against earthquake magnitude.

Choosing appropriate IMs as predictors is one of the key aspects for developing Newmark displacement models. Among the employed predictors in the existing models, PGA seems to be a necessary IM, because PGA > a_c is an essential prerequisite for triggering sliding in the Newmark model. The other IMs, such as Ia, PGV, Sa(T = 1 s), could be

Table 3
Summary of various weighting schemes in logic-tree approach.

Model name	Equal weights	Expert 1 weight	Expert 2 weights	Expert 3 weights	Expert 4 weights	Random weights
[PGA] AM88	0.14	0.1	0.1	0.33	0.05	0.29
[PGA Ia] R00	0.14	0.1	0.2	0	0.2	0.28
[PGA Ia] J07	0.14	0.16	0.2	0	0.05	0.11
[PGA M_w] BT07	0.14	0.16	0.1	0.33	0.2	0.19
[PGA Ia] RS08	0.14	0.16	0.2	0	0.15	0.03
[PGA M_w] RS09	0.14	0.16	0.1	0.33	0.15	0.04
[Ia] HL11	0.14	0.16	0.1	0	0.2	0.05

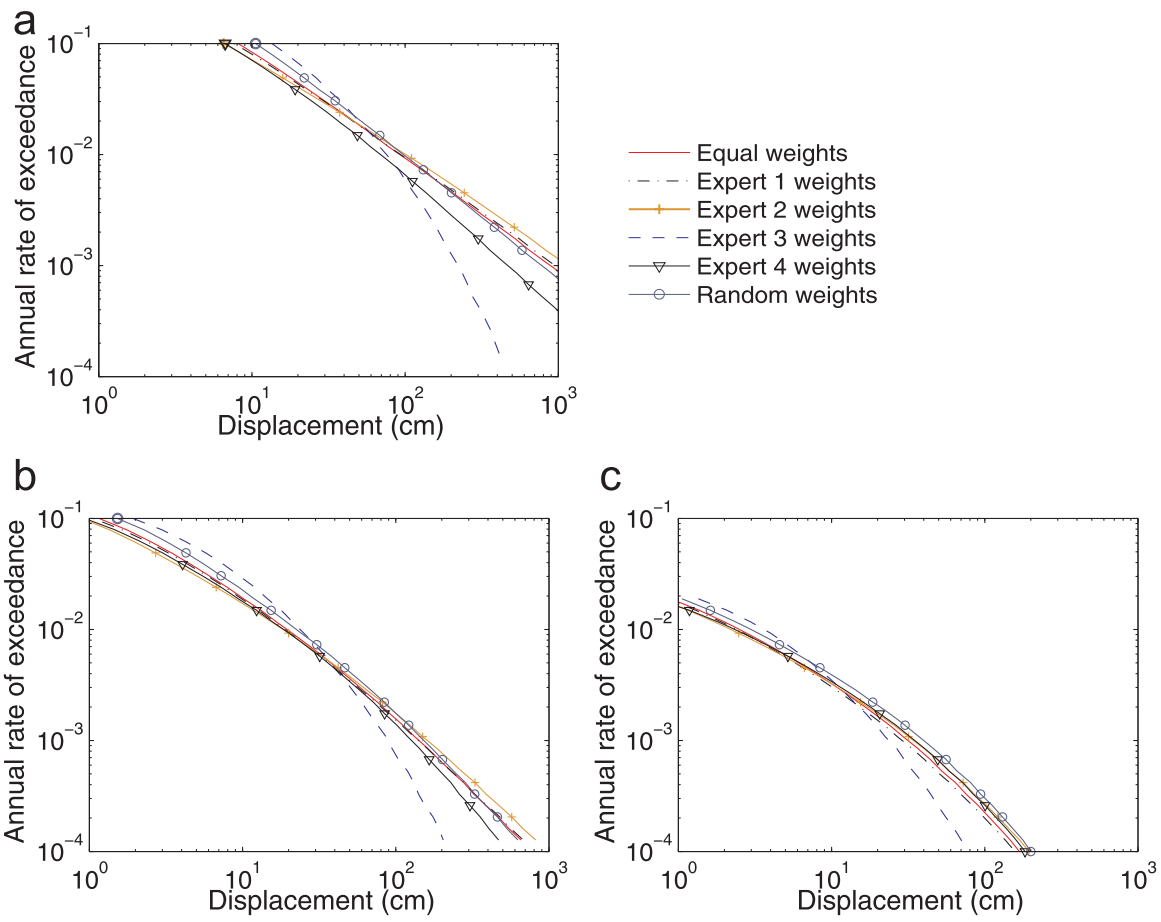

Fig. 11. Displacement hazard curves using six weighting schemes shown in Table 3 for three cases: (a) a_c = 0.05 g, (b) a_c = 0.1 g and (c) a_c = 0.2 g.

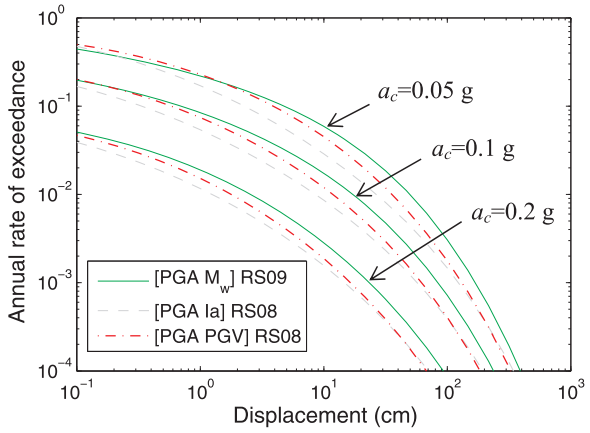

Fig. 12. Comparison of displacement hazard curves.

used together with PGA to quantify different characteristics of the ground motion. It is beyond this paper's scope to distinguish which IM is superior in association with PGA, because we believe more elaborate work needs to be done. However, we do demonstrate that three [PGA Ia] models provide quite differed displacement hazard curves. On the other hand, displacement hazard curves developed from [PGA Ia] and [PGA PGV] models can be quite consistent. Interestingly, these models were developed by the same researchers.

Finally, several illustrative examples are provided to highlight the importance of quantifying model uncertainties and variabilities in the fully probabilistic displacement hazard analysis within a logic-tree framework. The results show that the model uncertainties in the GMPEs and Newmark displacement models are significant. Sensitivity analysis indicates that different weighting criterion may not significantly affect the hazard curves as the results may be dominated by models with the highest estimates (which may be outliers). Instead, it is more vital to select appropriate GMPEs and Newmark displacement models in the logic-tree framework. Attention should be paid to the applicable range and regional preference of these models.

It is worth mentioning that, most recently, a one-step model [7] is proposed to predict Newmark displacement directly based on seismological parameters rather than any IM. The one-step model can greatly simplify the analytical procedure and computational cost of fully probabilistic Newmark displacement analysis. Furthermore, with recent advancement in simulation-based seismic analysis, it is also possible to directly calculate Newmark displacements based on a large number of simulated strong-motion waveforms without the need of a Newmark displacement prediction model. For example, recent work on stochastic simulation of ground motions [42–44] shed light in this direction.

Acknowledgments

The authors acknowledge financial support from Hong Kong Research Grants Council General Research Fund no. 16213615, Theme-based Research fund T22-603/15N and DAG11EG03G.

References

[1] Newmark NM. Effects of earthquakes on dams and embankments. Géotechnique 1965;15(2):139–60.
[2] Saygili G, Rathje EM. Probabilistically based seismic landslide hazard maps: an application in Southern California. Eng Geol 2009;109(3):183–94.
[3] Jibson RW, Michael JA. Maps showing seismic landslide hazards in Anchorage,

Alaska. U.S. Geological Survey Scientific Investigations Map 3077. 2 sheets (scale 1:25, 000). Pamphlet; 2009. p. 11.
[4] Pradel D, Smith PM, Stewart JP, Raad G. Case history of landslide movement during the Northridge earthquake. J Geotech Geoenviron Eng 2005;131:1360–9.
[5] Jibson RW. Methods for assessing the stability of slopes during earthquakes - a retrospective. Eng Geol 2011;122(1):43–50.
[6] Du W, Wang G. Fully probabilistic seismic displacement analysis of spatially distributed slopes using spatially correlated vector intensity measures. Earthq Eng Struct Dyn 2014;43(5):661–79.
[7] Du W, Wang G. A one-step Newmark displacement model for probabilistic seismic slope displacement hazard analysis. Eng Geol 2016;205:12–23.
[8] Ambraseys NN, Menu JM. Earthquake-induced ground displacements. Earthq Eng Struct Dyn 1988;16(7):985–1006.
[9] Jibson RW. Regression models for estimating coseismic landslide displacement. Eng Geol 2007;91:209–18.
[10] Saygili G, Rathje EM. Empirical predictive models for earthquake-induced sliding displacements of slopes. J Geotech Geoenviron Eng 2008;134(6):790–803.
[11] Hsieh SY, Lee CT. Empirical estimation of Newmark displacement from the Arias intensity and critical acceleration. Eng Geol 2011;2011(122):34–42.
[12] Arias A. Measure of earthquake intensity. In: Hansen RJ, editor. Seismic design for nuclear power plants. Cambrige, MA: Massachusetts Institute of Technology press; 1970. p. 438–83.
[13] Wang G. Efficiency of scalar and vector intensity measures for seismic slope displacements. Front Struct Civil Eng 2012;6(1):44–52.
[14] Cornell CA, Luco N. Ground motion intensity measures for structural performance assessment at near-fault sites. In: Proceedings of the U.S.-Japan Joint Workshop and Third Grantees Meeting, U.S. - Japan Cooperative Research on Urban EQ. Disaster Mitigation, Seattle; 2001.
[15] Douglas J. Consistency of ground-motion predictions from the past four decades. Bull Earthq Eng 2010;8(6):1515–26.
[16] Douglas J. Consistency of ground-motion predictions from the past four decades: peak ground velocity and displacement, Arias intensity and relative significant duration. Bull Earthq Eng 2012;10(5):1339–56.
[17] Douglas J, Akkar S, Ameri G, Bard PY, Bindi D, Bommer JJ, Bora SS, Cotton F, Derras B, Hermkes M, Kuehn NM. Comparisons among the five ground-motion models developed using RESORCE for the prediction of response spectral accelerations due to earthquakes in Europe and the Middle East. Bull Earthq Eng 2014;12(1):341–58.
[18] Benjamin JR, Cornell CA. Probability, statistics, and decision for civil engineers. New York NY: McGraw-Hill; 1970.
[19] Kulkarni RB, Youngs RR, Coppersmith KJ. Assessment of confidence intervals for results of seismic hazard analysis, in In: Proceedings of the 8th World Conference on Earthquake Engineering, San Francisco, California, 21–28 July, 263-270; 1984.
[20] Rathje EM, Saygili G. Probabilistic assessment of earthquake-induced sliding displacements of natural slopes. Bull NZ Soc Earthq Eng 2009;42(1):18.
[21] Romeo R. Seismically induced landslide displacements: a predictive model. Eng Geol 2000;58(3):337–51.
[22] Watson-Lamprey J, Abrahamson N. Selection of ground motion time series and limits on scaling. Soil Dyn Earthq Eng 2006;26(5):477–82.
[23] Bray JD, Travasarou T. Simplified procedure for estimating earthquake-induced deviatoric slope displacements. J Geotech Geoenviron Eng 2007;133:381–92.
[24] Abrahamson NA, Silva WJ. Summary of the Abrahamson & Silva NGA ground-motion relations. Earthq Spectra 2008;24(1):67–97.
[25] Boore DM, Atkinson GM. Ground-motion prediction equations for the average horizontal component of PGA, PGV and 5%-damped PSA at spectral periods between 0.01s and 10s. Earthq Spectra 2008;24(1):99–138.
[26] Campbell KW, Bozorgnia Y. NGA ground motion model for the geometric mean horizontal component of PGA, PGV, PGD and 5% damped linear elastic response spectra for periods ranging from 0.1 to 10 s. Earthq Spectra 2008;24(1):139–71.
[27] Chiou B, Youngs RR, An NGA. model for the average horizontal component of peak ground motion and response spectra. Earthq Spectra 2008;24(1):173–215.
[28] Travasarou T, Bray JD, Abrahamson NA. Empirical attenuation relationship for Arias Intensity. Earthq Eng Struct Dyn 2003;32(7):1133–55.
[29] Foulser-Piggott R, Stafford PJ. A predictive model for Arias intensity at multiple sites and consideration of spatial correlations. Earthq Eng Struct Dyn 2012;41(3):431–51.
[30] Campbell KW, Bozorgnia Y. A comparison of ground motion prediction equations for Arias intensity and cumulative absolute velocity developed using a consistent database and functional form. Earthq Spectra 2012;28(3):931–41.
[31] Baker JW, Jayaram N. Correlation of spectral acceleration values from NGA ground motion models. Earthq Spectra 2008;24(1):299–317.
[32] Baker JW. Correlation of ground motion intensity parameters used for predicting structural and geotechnical response. In: Proceedings of the Tenth International Conference on Application of Statistics and Probability in Civil Engineering. Vol. 8; 2007.
[33] Bradley BA. Empirical correlations between peak ground velocity and spectrum-based intensity measures. Earthq Spectra 2012;28(1):17–35.
[34] Rathje EM, Saygili G. Probabilistic seismic hazard analysis for the sliding displacement of slopes: scalar and vector approaches. J Geotech Geoenviron Eng 2008;134(6):804–14.
[35] Bazzurro P, Cornell CA. Vector-valued probabilistic seismic hazard znalysis (VPSHA). Seventh U.S. National In: Proceedings of the Conference on Earthquake Engineering, EERI, Vol. II; 1313–1322; 2002.
[36] Bommer JJ, Scherbaum F, Bungum H, Cotton F, Sabetta F, Abrahamson NA. On the use of logic trees for ground-motion prediction equations in seismic-hazard analysis. Bull Seismol Soc Am 2005;95(2):377–89.
[37] Bommer JJ, Scherbaum F. The use and misuse of logic trees in probabilistic seismic hazard analysis. Earthq Spectra 2008;24(4):997–1009.
[38] Bommer JJ. Challenges of building logic trees for probabilistic seismic hazard analysis. Earthq Spectra 2012;28(4):1723–35.
[39] Musson R. On the nature of logic trees in probabilistic seismic hazard assessment. Earthq Spectra 2012;28(3):1291–6.
[40] Sabetta F, Lucantoni A, Bungum H, Bommer JJ. Sensitivity of PSHA results to ground motion prediction relations and logic-tree weights. Soil Dyn Earthq Eng 2005;25(4):317–29.
[41] Delavaud E, Cotton F, Akkar S, Scherbaum F, Danciu L, Beauval C, Drouet S, Douglas J, Basili R, Sandikkaya MA, Segou M, Faccioli E, Theodoulidis N. Toward a ground-motion logic tree for probabilistic seismic hazard assessment in Europe. J Seismol 2012;16(3):451–73.
[42] Yamamoto Y, Baker JW. Stochastic model for earthquake ground motion using wavelet packets. Bull Seismol Soc Am 2013;103(6):3044–56.
[43] Huang D, Wang G. Region-specific spatial cross-correlation model for stochastic simulation of regionalized ground-motion time histories. Bull Seismol Soc Am 2015;105(1):272–84.
[44] Huang D, Wang G. Stochastic simulation of regionalized ground motions using wavelet packet and cokriging analysis. Earthq Eng Struct Dyn 2015;44:775–94.